CHEMISTRY
A European Journal

A Journal of
ChemPubSoc Europe

Accepted Article

Title: "Turn-On" Activatable AIE Dots for Tumor Hypoxia Imaging

Authors: Tianhao Xue, Xiangqian Jia, Jilei Wang, Jingyuan Xiang, Wei Wang, Juanjuan Du, and Yaning He

To be cited as: *Chem. Eur. J.* 10.1002/chem.201902296

Link to VoR: http://dx.doi.org/10.1002/chem.201902296

Supported by
ACES

WILEY-VCH

"Turn-On" Activatable AIE Dots for Tumor Hypoxia Imaging

Tianhao Xue[⊥],[a] Xiangqian Jia[⊥],[b] Jilei Wang,[a] Jingyuan Xiang,[a] Wei Wang, [a] Juanjuan Du*[b] and Yaning He*[a]

[⊥] These authors contributed equally to this work

Abstract: This communication reported a hypoxia-responsive fluorescence probe of amphiphilic PEGylated azobenzene caged tetraphenylethene (TPE) for tumor cell imaging, which possessed excellent solubility in aqueous medium due to the easily forming micelles by self-assembly. Due to the fluorescence resonance energy transfer (FRET) process, the fluorescence of the azobenene caged AIE fluorogen will be quenched efficiently. When cultured with tumor cells, the azo-bond is reduced under hypoxia conditions and the fluorescence of AIE fluorogen recovers dramatically. Besides using UV light, near-infrared (NIR) light can also be used as the excited light resource to generate the fluorescence due to the two photon fluorescence imaging process.

Different from the conventional fluorophores that were self-quenched in an aggregation state, aggregation-induced emission (AIE) fluorogens emit strong fluorescence in aggregation states, due to the restriction of intramolecular motions. [1-3] For example, the tightly packed AIEgens in the core of AIE nanoparticles yields high fluorescence brightness, which can be 10−40 times brighter than that of quantum dots. [4,5] Additionally, AIE aggregates show an excellently linear concentration-dependent increase in brightness and high resistance to photobleaching. [6] Moreover, due to the large two-photon absorption cross-sections, AIE aggregates are especially suitable for two-photon fluorescence imaging. [7] Therefore, AIE fluorogens have recently become appealing fluorescence agents for bioimaging. Among them, AIE dots are nanoparticles with an AIE fluorogen (AIEgens) core and biocompatible materials as the shell. [6-8] Due to the high brightness and biocompatibility, the AIE dots have gained great success in bioimaging. However, studies on AIE dot based biosensors remain rare. [9] Developing novel environment-sensitive AIE dots is in need to further expand the application of these exceptional fluorescence nanoaggregates. Therefore, in this work, we present an activatable AIE dot (aAIE dot), which is an organic dot that can be activated to emit AIE fluorescence in response to environmental cues.

[a] T.H. Xue, J.L. Wang, J.Y. Xiang, W. Wang, Dr. Y.N. He
Department of Chemical Engineering
Key Laboratory of Advanced Materials (MOE)
Tsinghua University, Beijing, 100084, China.
E-mail: heyaning@mail.tsinghua.edu.cn
[b] X.Q. Jia, Dr. J.J. Du
School of Pharmaceutical Sciences
Tsinghua University, Beijing, 100084, China.
Email: dusps@mail.tsinghua.edu.cn

Supporting information for this article is given via a link at the end of the document.

Hypoxia is among the most important features of malignant tumors. [10-12] As the tumor grows in an exaggerated way, interior cells of the tumor rapidly outgrow their blood supply, leading to a reduced oxygen concentration in the intratumoral microenvironment. Furthermore, tumor hypoxia alters cancer cell metabolism and contributes to cancer cell invasion, metastasis, and therapy resistance. Therefore, sensing tumor hypoxia is particularly important for tumor diagnosis and prognosis. [13-15]

Azobenzene derivatives with intense absorption bands in the UV-visible light region often serve as non-fluorescent energy acceptors to quench fluorophores in proximity. [16] The azobenzene quenched system has been used for proteolysis and nucleic acid hybridization detection. [17] What's more, the azobenzene chromophore can be reduced efficiently in the hypoxic microenvironment, [18-24] to recover the fluorescence of the system. Therefore, the reducible azobenzene-containing fluorophores can be used as ''off–on'' fluorescent probes for the detection of tumor hypoxia. [14, 25-31]

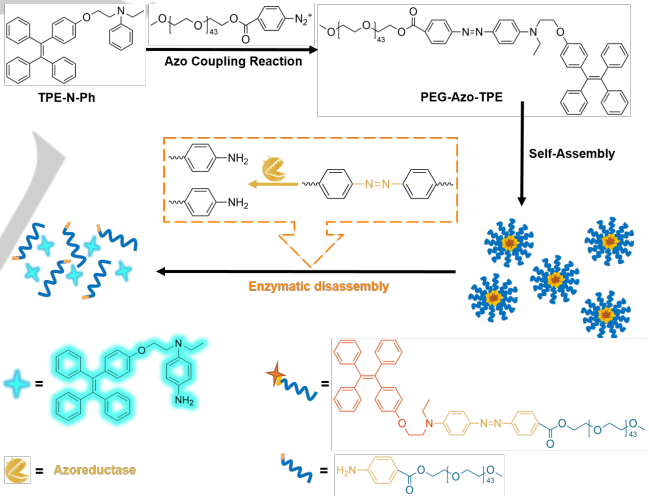

Scheme 1. Fabrication of activatable polymeric AIE aggregates via self-assembly in aqueous solution.

Although conventional fluorophores caged by azobenzene have been explored as hypoxia-sensitive fluorescent probes, the azobenzene caged AIE fluorescent probe has not been reported yet. In this communication, we reported a "turn-on" hypoxia-responsive fluorescence probe of PEGylated azobenzene caged tetraphenylethene (TPE) (Scheme 1). Due to the amphiphilic chemical structure, this PEGylated azobenzene-TPE derivative can form nanoaggregates by self-assembly in the aqueous medium, yielding stable azobenzene-caged aAIE dots. The fluorescence of the azobenzene-caged AIE fluorogen will be

quenched efficiently because of fluorescence resonance energy transfer (FRET) process. In hypoxic tumor microenvironment, the overexpressed azoreductase cleaves the azobenzene moieties, recovering the fluorescence of the AIE fluorogen. In addition, we have demonstrated that this "turn-on" fluorescent probe can be used for two-photon imaging with near-infrared (NIR) light as the excitation light source.

The hypoxia-responsive fluorescence probe of amphiphilic PEGylated azobenzene caged TPE (PEG-Azo-TPE) was synthesized by the macromolecular azo coupling reaction between a PEG diazonium salt and a TPE modified aniline (Scheme 1, the detailed synthesis route is shown in Figure S1). The macromolecular azo coupling reaction has been proved to be a very efficient method to prepare amphiphilic diblock copolymers. [32-35] Here, we use the macromolecular azo coupling reaction to obtain the designed PEG-Azo-TPE. A diazonium salt of PEG-NH_2 was prepared by adding an aqueous solution of sodium nitrite into a mixture of PEG-NH_2, HCl (36%) and H_2O. Then the diazonium salt of PEG-NH_2 was added dropwise into the solution of TPE modified aniline to afford PEG-Azo-TPE. The synthetic details of PEG diazonium salts and TPE modified aniline are shown in the supporting materials. The ^1H NMR spectra of the prepared PEG-Azo-TPE is shown in Figure S2. The characteristic peaks corresponding to the protons of the azobenzene caged TPE moiety (6.63-8.12 ppm) and the PEG chain (3.50-3.70 ppm) indicate the successful construction of PEG-Azo-TPE. Figure S3 shows the gel permeation chromatography (GPC) of PEG monomethyl ether and PEG-Azo-TPE, demonstrating the molecular weight gain after conjugating the Azo-TPE groups to the PEG chain. Figure S4 reveals the UV−visible absorption spectrum of PEG-Azo-TPE. The obvious absorption in the visible region (λ_{max} = 438 nm) can be attributed to the typical absorption behavior of the pseudo-stilbene type of azo chromophores corresponding to the π-π* transition. Collectively, these evidences prove that PEG-Azo-TPE is successfully synthesized.

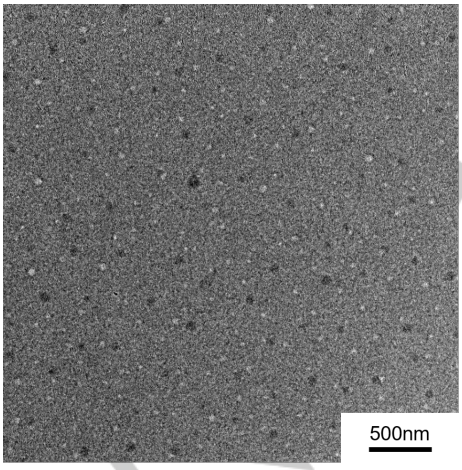

Figure 1. Typical TEM image of the self-assembly nanoparticles of PEG-Azo-TPE in aqueous solution.

The resulted PEG-Azo-TPE is amphiphilic, with a hydrophobic TPE head and a hydrophilic PEG tail linked by the azobenzene linker. Thus, this amphiphilic macromolecule can be self-assembled into micelles in aqueous solutions, yielding azobenzene-caged TPE aAIE dots stabilized by biocompatible PEG. The TEM image of the self-assembled aggregates is shown in Figure 1. Uniform nanoparticles with a mean diameter around 90 nm were obtained (estimated statistically from the TEM image). This observation is consistent with the results of the dynamic light scattering (DLS) measurement (Figure S5).

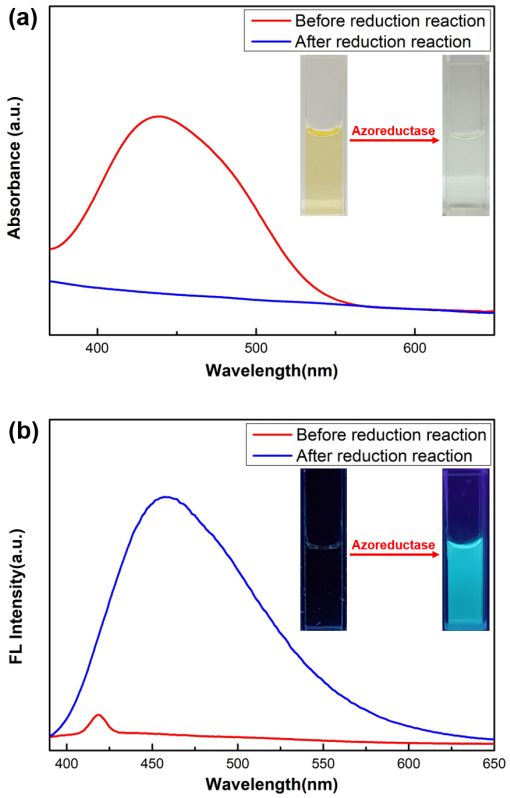

Figure 2. UV-visible absorption (a) and fluorescence (b) spectra of the self-assembled nanoaggregates in aqueous solution before and after enzymatic reduction reaction in the hypoxic condition (the inserts represent the photographs of the aggregate aqueous solutions before and after the reduction reaction).

It has been reported that the azo bond (N=N) in azobenzene compounds can be efficiently reduced by azoreductase treatment in the hypoxic condition. [22, 24, 36-37] To test whether the cleavage of PEG-Azo-TPE can reactivate TPE fluorescence, the UV-visible and fluorescent spectra of PEG-Azo-TPE self-assembly aggregates were measured before and after enzyme treatment in hypoxic condition (Figure 2). The absorption peak in the visible region attributed to the pseudo-stilbene type azo chromophores disappeared after the reduction reaction (Figure 2(a)), verifying the cleavage of the azobenzene chromophores. In addition, the fluorescence spectrum of PEG-Azo-TPE showed no observable emission with excitation light of 365 nm red line of

Figure 2(b)), validating our hypothesis that the azobenzene moiety effectively quenched the fluorescence of the TPE dots. After the treatment with enzyme, the fluorescence of TPE at 465 nm re-appeared when excited with 365 nm light (blue line of Figure 2(b)). The ON/OFF ratio of the fluorescence emission was more than 25 fold. Strong fluorescence could be observed by naked eyes, which was shown in the insert of Figure 2(b). The reduction product TPE-NH_2 has been detected by mass spectrometry (Figure S6). The destruction of the micelles also can be observed after the enzyme treatment (Figure S7). All of above results demonstrated that PEG-Azo-TPE nanoparticles could be used as a "turn-on" fluorescence probe triggered by azoreductase.

The activatable fluorescence can be also observed with two-photon excitation with near-infrared (NIR) light. NIR light penetrates deeper into the tissue and is less detrimental to the biomolecules. Thus, two-photon fluorescence imaging may provide a possible optical window for in-vivo imaging with deep tissue penetration and minimal phototoxicity to the living cells. Figure S8 shows the two-photon fluorescence spectrum of the PEG-Azo-TPE aggregates in aqueous solution after the enzyme treatment. No fluorescence could be observed before the reduction reaction due to the FRET-mediated quenching. After the enzyme treatment, the emission peak at 465 nm was observed when excited with 760 nm light, in consistent with the fluorescence emission of TPE dots.

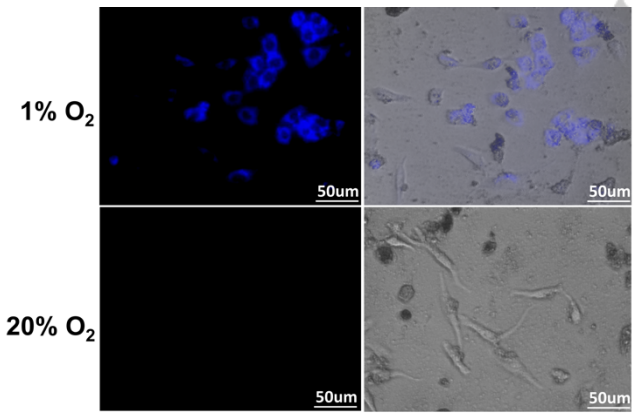

Figure 3. Microscopy images of adherent A549 cells treated with PEG-Azo-TPE probes under normoxia (20% O_2) and hypoxia (1% O_2).

As the azoreductases are reportedly over-expressed in hypoxic cancer cells, [38-41] we further tested whether PEG-Azo-TPE aggregates can be reduced to restore TPE fluorescence in hypoxic tumor cell cultures. Figure 3 shows the fluorescence images of adherent A549 cells after the incubation with PEG-Azo-TPE under different oxygen concentrations. A549 cells treated with the PEG-Azo-TPE nanoparticles under normoxic conditions (20% v/v O_2) show negligible background fluorescence. This can be attributed to the negligible expression of azoreductase in A549 cells under normoxic conditions. Under normoxic conditions, the probe itself emits very weak fluorescence, leading to no observable fluorescence in the cell culture. In contrast, A549 cells treated with the PEG-Azo-TPE nanoparticles under hypoxic conditions (1% v/v O_2) produced dramatically increased fluorescence. This is due to the generation of upregulated azoreductase in tumor hypoxia mediated the cleavage of the azobenzene linkage to restore the fluorescence of TPE dots. And we confirmed the existence of azoreductase in cells culture supernatant by using a continuous spectrophotometric rate assay (Figure S9). The determination details are shown in the supporting materials. These results clearly indicate that the PEG-Azo-TPE can be utilized to distinguish the hypoxic status from tumor tissue via the detection of endogenous azoreductase.

In the cytotoxicity experiments, we incubated PEG-Azo-TPE with HeLa cells under normoxic and hypoxic environment. In both conditions, HeLa cells show high viability (higher than 80%) in PEG-Azo-TPE solutions with concentrations up to 0.8 mg/mL (Figure S10), indicating PEG-Azo-TPE has minimal cytotoxicity against HeLa cells.

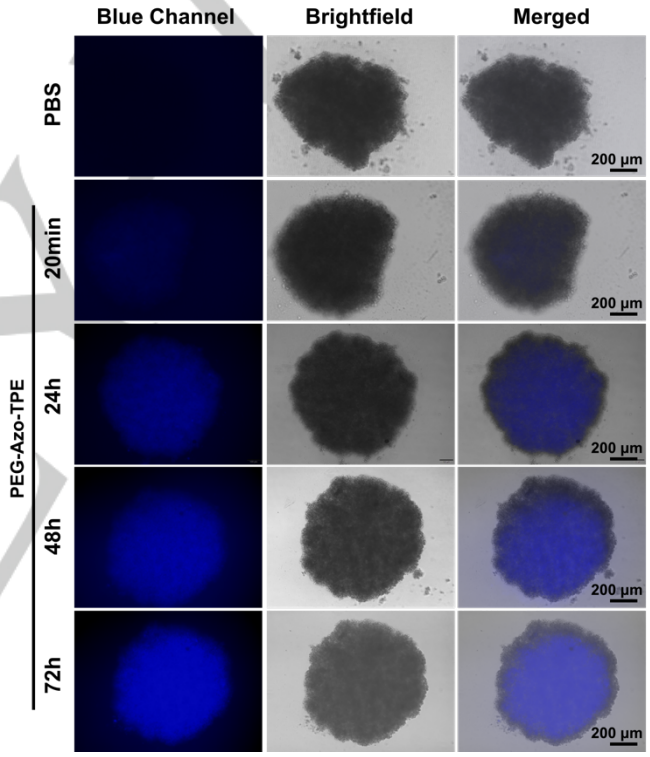

Figure 4. Fluorescence microscopy images of Hela multicellular tumor spheroids (MCTS) incubated with PBS or PEG-Azo-TPE.

The multicellular tumor spheroid (MCTS) model, a well-established 3D cell culture method, has been proved superiority over monolayer cell culture models to recapitulate *in vivo* tumor growth. [42, 43] In particular, MCTS mimics *in vivo* tumor models by developing hypoxic and apoptotic/necrotic areas as a consequence of the formation of oxygen and nutrient gradients. [44, 45] To investigate whether PEG-Azo-TPE can be used to image the hypoxia area in the MCTS, we incubated PEG-Azo-TPE with preformed MCTS of HeLa cells for different time. Figure 4 shows the fluorescence microscopy images of HeLa MCTS with or without the treatment of PEG-Azo-TPE. In comparison to the HeLa MCTS treated with PBS, HeLa MCTS

treated with PEG-Azo-TPE shows significantly higher fluorescence emission. Moreover, the fluorescence intensity in the MCTS gradually increased with prolonged incubation time up to 72 hours. The time-dependent increase in fluorescence intensity may be attributed to the sustained release of the TPE AIE fluorogen from the PEG-Azo-TPE aggregates. The MCTS formed with A549 cells were used to verify this phenomenon. Figure S11 shows the fluorescence images of A549 MCTS after the incubation with PBS or PEG-Azo-TPE. Similarly, significantly higher fluorescence was observed in the MCTS treated with PEG-Azo-TPE in comparison to the control group. These observations demonstrated that PEG-Azo-TPE serves as a "turn-on" fluorescence probe to detect hypoxia area in tumor 3D culture.

The two-photon fluorescence imaging was carried out with the HeLa MCTS. Figure 5 represents the microscopy images of HeLa MCTS treated with PEG-Azo-TPE nanoparticles excited with 760nm laser. Strong fluorescence can be observed after the HeLa MCTS was incubated with the PEG-Azo-TPE for 72h. On the contrary, no detectable fluorescence was observed in HeLa MCTS without PEG-Azo-TPE treatment. This experiment verified that PEG-Azo-TPE could be used as a hypoxia probe in two-photon fluorescence imaging.

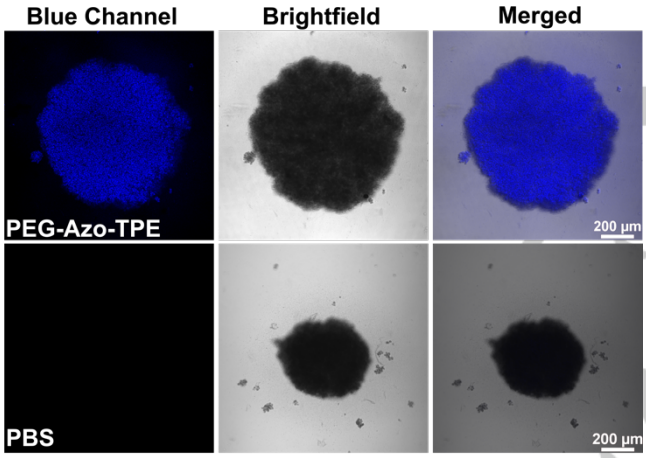

Figure 5. Microscopy images of HeLa multicellular tumor spheroids (MCTS) treated with PEG-Azo-TPE probes excited with 760nm light. The HeLa multicellular tumor spheroids (MCTS) were incubated with PBS and PEG-Azo-TPE for 72h.

In summary, a hypoxia-responsive "turn-on" fluorescence probe of PEGylated azobenzene-caged tetraphenylethene (PEG-Azo-TPE) for tumor hypoxia imaging was reported. This amphiphilic PEGylated macromolecule forms nano-scale PEG-stabilized azobenene-caged aAIE dots by self-assembly in the aqueous medium. The fluorescence of the azobenene-caged aAIE dots is efficiently quenched, due to the FRET-mediated quenching. When incubated with tumor cells, the azo-bond is reduced under hypoxia conditions to recover fluorescence of the core AIE fluorogen. In addition to UV light, near-infrared (NIR) light can be used as the excitation light source for two-photon fluorescence imaging with PEG-Azo-TPE as the hypoxia probe. As AIE aggregates have distinct advantages over other fluorophores, this work opens up new possibilities for tumor imaging with AIE fluoreogens, such as deep-tissue imaging. Moreover, nanoparticles are reported to accumulate in some tumor tissues by the enhanced permeability and retention (EPR) effect. The nano-scale PEG-Azo-TPE dots may have further advantages over conventional small molecular probes. Future research is ongoing to explore the unique behavior of the nano-scale hypoxia probe.

Acknowledgements

The authors gratefully acknowledge financial support from the National Key Research and Development Program of China (Grant Nos. 2017YFA0701303, 2018YFA0209700), and the National Natural Science Foundation of China (Grant Nos. 51873097 and 21674058).

Keywords: hypoxia • fluorescence probe • self-assembly • azobenzene • AIE

[1] D. Ding, K. Li, B. Liu, B. Z. Tang, *Accounts Chem Res* **2013**, *46*, 2441-2453.
[2] J. Mei, Y. N. Hong, J. W. Y. Lam, A. J. Qin, Y. H. Tang, B. Z. Tang, *Adv Mater* **2014**, *26*, 5429-5479.
[3] X. Gu, R. T. K. Kwok, J. W. Y. Lam, B. Z. Tang, *Biomaterials* **2017**, *146*, 115-135.
[4] K. Li, W. Qin, D. Ding, N. Tomczak, J. L. Geng, R. R. Liu, J. Z. Liu, X. H. Zhang, H. W. Liu, B. Liu, B. Z. Tang, *Sci Rep-Uk* **2013**, *3*, 1150.
[5] D. Wang, J. Qian, W. Qin, A. J. Qin, B. Z. Tang, S. L. He, *Sci Rep-Uk* **2014**, *4*, 4279.
[6] G. X. Feng, B. Liu, *Accounts Chem Res* **2018**, *51*, 1404-1414.
[7] X. Lou, Z. Zhao, B. Z. Tang, *Small* **2016**, *12*, 6430-6450.
[8] S. J. Chen, H. Wang, Y. N. Hong, B. Z. Tang, *Mater Horiz* **2016**, *3*, 283-293.
[9] X. Wang, Y. Y. Yang, Y. P. Zhuang, P. Y. Gao, F. Yang, H. Shen, H. X. Guo, D. C. Wu, *Biomacromolecules* **2016**, *17*, 2920-2929.
[10] H. K. Eltzschig, P. Carmeliet, *New Engl J Med* **2011**, *364*, 656-665.
[11] D. M. Gilkes, G. L. Semenza, D. Wirtz, *Nat Rev Cancer* **2014**, *14*, 430-439.
[12] S. K. Parks, Y. Cormerais, J. Pouyssegur, *J Physiol-London* **2017**, *595*, 2439-2450.
[13] Y. Zeng, J. W. Ma, S. J. Zhang, D. C. Wu, *Curr Med Chem* **2016**, *23*, 1775-1800.
[14] T. Thambi, J. H. Park, D. S. Lee, *Chem Commun* **2016**, *52*, 8492-8500.
[15] C. S. Wang, Z. H. Wang, T. Zhao, Y. Li, G. Huang, B. D. Sumer, J. M. Gao, *Biomaterials* **2018**, *157*, 62-75.
[16] J. T. Wu, Y. Tan, Y. H. Xie, Y. Wu, R. Zhao, Y. Y. Jiang, C. Y. Tan, *Chem Commun* **2013**, *49*, 11379-11381.
[17] J. W. J. Li, X. H. Fang, S. M. Schuster, W. H. Tan, *Angew Chem Int Edit* **2000**, *39*, 1049-1052.
[18] S. H. Lee, E. Moroz, B. Castagner, J. C. Leroux, *J Am Chem Soc* **2014**, *136*, 12868-12871.
[19] S. Li, J. L. Wang, J. J. Shen, B. Wu, Y. N. He, *Acs Macro Lett* **2018**, *7*, 437-441.
[20] J. L. Wang, B. Wu, S. Li, Y. N. He, *J Polym Sci Pol Chem* **2017**, *55*, 2450-2457.
[21] P. Kulkarni, M. K. Haldar, S. You, Y. Choi, S. Mallik, *Biomacromolecules* **2016**, *17*, 2507-2513.
[22] J. Y. Rao, C. Hottinger, A. Khan, *J Am Chem Soc* **2014**, *136*, 5872-5875.
[23] F. Perche, S. Biswas, T. Wang, L. Zhu, V. P. Torchilin, *Angew Chem Int Edit* **2014**, *53*, 3362-3366.
[24] J. Y. Rao, A. Khan, *J Am Chem Soc* **2013**, *135*, 14056-14059.

[25] W. Piao, S. Tsuda, Y. Tanaka, S. Maeda, F. Y. Liu, S. Takahashi, Y. Kushida, T. Komatsu, T. Ueno, T. Terai, T. Nakazawa, M. Uchiyama, K. Morokuma, T. Nagano, K. Hanaoka, *Angew Chem Int Edit* **2013**, *52*, 13028-13032.
[26] K. Kiyose, K. Hanaoka, D. Oushiki, T. Nakamura, M. Kajimura, M. Suematsu, H. Nishimatsu, T. Yamane, T. Terai, Y. Hirata, T. Nagano, *J Am Chem Soc* **2010**, *132*, 15846-15848.
[27] W. Piao, K. Hanaoka, T. Fujisawa, S. Takeuchi, T. Komatsu, T. Ueno, T. Terai, T. Tahara, T. Nagano, Y. Urano, *J Am Chem Soc* **2017**, *139*, 13713-13719.
[28] J. Li, Y. Yuan, G. S. Zeng, X. Li, Z. Yang, X. Z. Li, R. C. Jiang, W. B. Hu, P. F. Sun, Q. Wang, X. M. Lu, Q. L. Fan, W. Huang, *Polym Chem-Uk* **2016**, *7*, 6890-6894.
[29] S. Y. Lim, K. H. Hong, D. I. Kim, H. Kwon, H. J. Kim, *J Am Chem Soc* **2014**, *136*, 7018-7025.
[30] Q. Cai, T. Yu, W. P. Zhu, Y. F. Xu, X. H. Qian, *Chem Commun* **2015**, *51*, 14739-14741.
[31] A. Chevalier, P. Y. Renard, A. Romieu, *Chem-Asian J* **2017**, *12*, 2008-2028.
[32] R. B. Wei, X. G. Wang, Y. N. He, *Eur Polym J* **2015**, *69*, 584-591.
[33] J. L. Wang, Y. Y. Ouyang, S. Li, X. G. Wang, Y. N. He, *Rsc Adv* **2016**, *6*, S7227-S7231.
[34] Y. N. He, W. He, D. Liu, T. H. Gu, R. B. Wei, X. G. Wang, *Polym Chem* **2013**, *4*, 402-406.
[35] Y. N. He, W. He, R. B. Wei, Z. Chen, X. G. Wang, *Chem Commun* **2012**, *48*, 1036-1038.
[36] J. Rao, A. Khan, *Polymer Chemistry* **2015**, 6, 686-690.
[37] K. Ito, M. Nakanishi, W. C. Lee, Y. Zhi, H. Sasaki, S. Zenno, K. Saigo, Y. Kitade, M. Tanokura, *J Biol Chem* **2008**, *283*, 13889-13896.
[38] A. Ryan, *Brit J Pharmacol* **2017**, *174*, 2161-2173.
[39] Y. Yang, Y. Zhang, Q. Y. Wu, X. L. Cui, Z. H. Lin, S. P. Liu, L. Y. Chen, *J Exp Clin Canc Res* **2014**, *33*.
[40] Z. L. Li, Y. Zhang, T. F. Jin, J. G. Men, Z. H. Lin, P. Qi, Y. S. Piao, G. H. Yan, *Bmc Cancer* **2015**, *15*.
[41] A. M. Lewis, M. Ough, M. M. Hinkhouse, M. S. Tsao, L. W. Oberley, J. J. Cullen, *Mol Carcinogen* **2005**, *43*, 215-224.
[42] C. R. Thoma, M. Zimmermann, I. Agarkova, J. M. Kelm, W. Krek, *Adv Drug Deliver Rev* **2014**, *69*, 29-41.
[43] D. V. LaBarbera, B. G. Reid, B. H. Yoo, *Expert Opin Drug Dis* **2012**, *7*, 819-830.
[44] S. Daster, N. Amatruda, D. Calabrese, R. Ivanek, E. Turrini, R. A. Droeser, P. Zajac, C. Fimognari, G. C. Spagnoli, G. Iezzi, V. Mele, M. G. Muraro, *Oncotarget* **2017**, *8*, 1725-1736.
[45] K. Klimkiewicz, K. Weglarczyk, G. Collet, M. Paprocka, A. Guichard, M. Sarna, A. Jozkowicz, J. Dulak, T. Sarna, C. Grillon, C. Kieda, *Cancer Lett* **2017**, *396*, 10-20.

10.1002/chem.201902296

WILEY-VCH

Entry for the Table of Contents (Please choose one layout)

COMMUNICATION

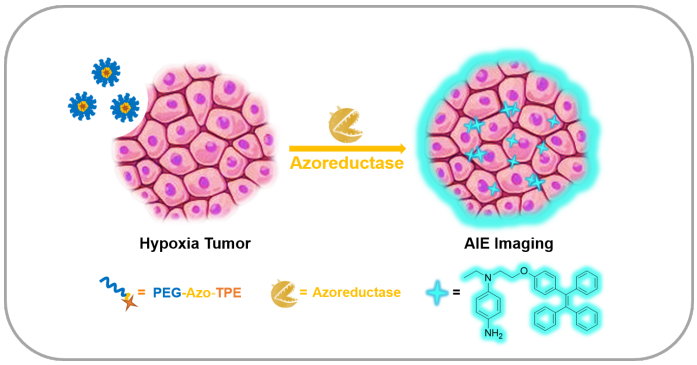

Tianhao Xue, Xiangqian Jia, Jilei Wang, Jingyuan Xiang, Wei Wang, Juanjuan Du and Yaning He **

Page No. – Page No.

"Turn-On" Activatable AIE Dots for Tumor Hypoxia Imaging

A Novel hypoxia-responsive fluorescence probe of amphiphilic PEGylated azobenzene caged tetraphenylethene for tumor cell imaging is reported. Besides using UV light, near-infrared (NIR) light can also be used as the excited light resource to generate the fluorescence due to the two photon fluorescence imaging process.